

DNA MECHANICS

Craig J. Benham

UC Davis Genome Center, University of California, Davis, California 95616;
email: cjbenham@ucdavis.edu

Steven P. Mielke

Biophysics Graduate Group, University of California, Davis, California 95616; and
Biomedical Division, L-448 Biosciences Directorate, Lawrence Livermore National
Laboratory, Livermore, California 94551

Key Words DNA topology, DNA supercoiling, DNA modeling, equilibria,
dynamics

■ **Abstract** We review the history of DNA mechanics and its analysis. We evaluate several methods to analyze the structures of superhelical DNA molecules, each predicated on the assumption that DNA can be modeled with reasonable accuracy as an extended, linearly elastic polymer. Three main approaches are considered: mechanical equilibrium methods, which seek to compute minimum energy conformations of topologically constrained molecules; statistical mechanical methods, which seek to compute the Boltzmann distribution of equilibrium conformations that arise in a finite temperature environment; and dynamic methods, which seek to compute deterministic trajectories of the helix axis by solving equations of motion. When these methods include forces of self-contact, which prevent strand passage and preserve the topological constraint, each predicts plectonemically interwound structures. On the other hand, the extent to which these mechanical methods reliably predict energetic and thermodynamic properties of superhelical molecules is limited, in part because of their inability to account explicitly for interactions involving solvent. Monte Carlo methods predict the entropy associated with supercoiling to be negative, in conflict with a body of experimental evidence that finds it is large and positive, as would be the case if superhelical deformations significantly disrupt the ordering of ambient solvent molecules. This suggests that the large-scale conformational properties predicted by elastomechanical models are not the only ones determining the energetics and thermodynamics of supercoiling. Moreover, because all such models that preserve the topological constraint correctly predict plectonemic interwinding, despite these and other limitations, this constraint evidently dominates energetic and thermodynamic factors in determining supercoil geometry. Therefore, agreement between predicted structures and structures obtained experimentally, for example, by electron microscopy, does not in itself provide evidence for the correctness or completeness of any given model of DNA mechanics.

CONTENTS

THE EARLY HISTORY OF DNA	22
The Large-Scale Structure of DNA	22
The Energetics of DNA Deformations	26
METHODS TO ANALYZE THE STRUCTURE OF SUPERHELICAL DNA	32
Mechanical Equilibrium Methods	33
Statistical Mechanical Methods	35
Dynamic Methods	41
CONCLUSIONS AND OPEN QUESTIONS	46
Determinants of Superhelical DNA Structure	46

THE EARLY HISTORY OF DNA

The central role of DNA in biological processes was first demonstrated by Oswald Avery, who showed that DNA is the molecule that carries genetic information (1). This observation motivated the investigation of DNA structure, which culminated in 1953 in Watson & Crick's model of DNA as a double helix (2). In this model, the molecule was posited to be composed of two sugar-phosphate backbones, with one of four nitrogenous bases (A, C, G, or T) attached to each sugar. Each backbone had a (5'-3') chemical directionality, with the two strands oriented in an antiparallel manner. Each base on one strand was complementarily paired with the opposing base on the other strand, A with T and G with C. The sequence of bases along the molecule encoded the genetic information, so complete information could be recovered from either strand. Although crystal structures of DNA were not available until 1979, considerable indirect evidence quickly suggested that the Watson-Crick model was essentially correct. So for the first 25 years of the investigation of DNA structure, the molecule was regarded as a uniform, straight, right-handed double helix with 10 base pairs per turn.

The Large-Scale Structure of DNA

DNA was originally assumed to be a linear molecule. It was commonly isolated in linear form, although the techniques by which it was extracted from cells were sufficiently crude as to fractionate the molecule into relatively short fragments. Eukaryotic chromosomes, which were known to both appear and genetically map as linear arrays of genes, were thought each to contain a single, linear DNA molecule. So it came as a surprise when Jacob & Wollman found the genetic map of the bacterium *Escherichia coli* to be circular (3). This circular structure was soon directly confirmed by electron microscopy (4), and a number of other naturally occurring DNAs, in particular, viral genomes and bacterial plasmids, were found also to be circular (5, 6). Later work has shown that the DNA within chromosomes is partitioned into loops, called topological domains, which are constrained in a manner functionally equivalent to circles, as is described below. So circularity, in fact, is

an essentially universal attribute of all biologically active DNAs, at least at some stages in their life cycles.

It was quickly appreciated that circularity introduces a significant constraint on DNA. Vinograd & Lebowitz were the first to understand the nature of this constraint (7). (The history of this discovery is described in Reference 8.) To close a DNA molecule into a circle one must join the ends of the strands. Because the strands have antiparallel orientations, and because the directionality of each strand must be conserved, each strand can only close by binding its ends together. So the circular molecule has a structure comprised of two interlinked circles. The alternative, that the end of each strand binds to the other strand to form a Moebius strip, is chemically forbidden. So a closed circular molecule is constrained by the constancy of its linking number Lk . If one strand is cut while the other remains continuously circular, the linking number no longer remains constant. This is the nicked circular structure. The loops within chromosome domains also have constant linking numbers because duplex rotations are forbidden at points of loop attachment.

The precise nature of the constraint imposed by circularity was first described by Vinograd & Lebowitz (9). The constancy of the linking number in a closed circular DNA (ccDNA) couples its large-scale supercoiled (tertiary) structure and helical duplex winding according to the equation

$$Lk = Tw + Wr. \quad (1)$$

Here Lk is the linking number (originally called the topological winding number α). Wr is the writhing number (originally called τ , the number of superhelical turns), a measure of the tertiary structure, and Tw is the total molecular twist (originally called β , the duplex winding number), which is the total number of duplex turns. According to this equation, in a closed circular molecule where Lk is fixed, the number of tertiary turns is coupled to the number of duplex turns; changing one forces compensating changes in the other, so their sum remains constant.

The mathematics underlying this relationship was investigated independently by several mathematicians. The linking number was first defined by Gauss, apparently in an unpublished analysis of the orbits of asteroids (10). Lk is expressed as a double integral over the pair of curves (for DNA the two strands of the duplex), having a form called a Gaussian integral, shown in Equation 2 below. Calugareanu first examined a relationship similar to Equation 1 above, although he was considering differential geometric attributes of a single closed curve with nowhere vanishing curvature, not a pair of curves (11). The integral geometry underlying Calugareanu's formula was further developed by Pohl (12). In 1969, Jim White, in his doctoral dissertation, presented the relationship given in Equation 1 and examined it in its full mathematical generality in any number of dimensions (13). The connection of this mathematics to DNA, which had been empirically discovered by Vinograd & Lebowitz in 1966, was only made from the mathematical side in 1971 by Fuller (14).

Each of the three quantities, Lk , Tw , and Wr , has attributes not shared by the others (15). The linking number Lk associated to a ccDNA is an integer topological

invariant; Lk is fixed as long as both strands remain covalently closed. In contrast, both Wr and Tw are geometric invariants, whose values can vary as the covalently closed DNA is continuously deformed. Wr is an attribute of the central axis curve of the DNA, whereas both Tw and Lk are properties of the pair of strands of the duplex. And most importantly, both Lk and Wr are interactive parameters; their values may be computed either by crossing algorithms or by Gaussian double integrals. If s_1 and s_2 parametrize the positions along strands 1 and 2 of the duplex, the tangent vectors to the strands at these positions are $\mathbf{T}(s_1)$ and $\mathbf{T}(s_2)$, $\mathbf{e}(s_1, s_2)$ is the unit vector pointing from position s_1 to s_2 , and $r(s_1, s_2)$ is their separation distance, then the linking number is given by the Gaussian double integral:

$$Lk = \frac{1}{4\pi} \int_0^L \int_0^L \frac{\mathbf{e} \cdot (\mathbf{T}(s_2) \times \mathbf{T}(s_1))}{r^2} ds_1 ds_2. \quad (2)$$

In contrast, Tw is an extensive parameter, whose value is given by integration of the intensive twist density, or local helicity, $\tau(s)$:

$$Tw = \frac{1}{2\pi} \int_0^L \tau(s) ds. \quad (3)$$

As discussed below, this difference in the types of these parameters greatly complicates the analysis and modeling of the mechanics and energetics of ccDNA.

In what follows, three types of circular molecules need to be distinguished. In nicked circular molecules, one strand is a covalently continuous circle and the other has been cut. So although the molecule appears circular, the constraint imposed by Equation 1 is not operative. The relaxed state of a closed circular DNA is a phenomenologically defined condition in which the molecule is as unstressed as possible, given closed circularity. The linking number characterizing the relaxed state is denoted Lk_0 . If Lk_0 is not an integer, the relaxed state is not precisely attainable by any closed molecule. A closed circular DNA is said to be superhelical if its linking number Lk differs from the relaxed value. Its superhelicity is described by the linking difference $\alpha = Lk - Lk_0$. From any superhelical state, a single strand cut produces a nicked circle, and a double strand cut produces a full-length linear molecule.

Lk , and hence superhelicity, is closely regulated in many organisms. Negative superhelicity is seen in most organisms, although some that live at high temperatures have positive superhelicities. Patterns of gene expression are known to change with superhelicity, which gives this phenomenon considerable biological importance.

Supercoiled DNA molecules can be sorted according to their linking numbers using gel electrophoresis. Otherwise identical molecules whose linking numbers differ by one migrate at different velocities, and hence can be distinguished (16). In this way, populations of molecules having identical linking numbers can be isolated. Two chemically identical circular DNA molecules that have the same value of Lk are said to be topoisomers.

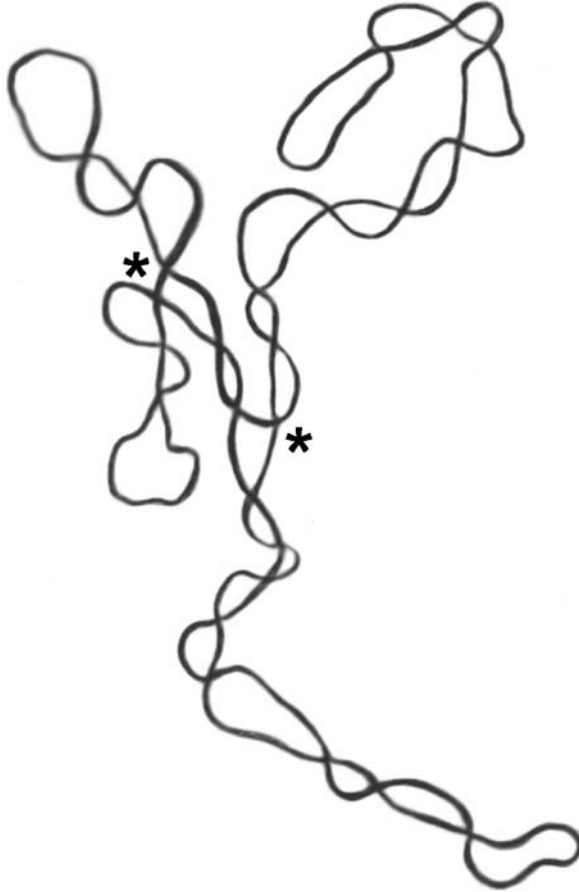


Figure 1 Branched, plectonemically interwound superhelical DNA [adapted from an electron micrograph of a seven-kilobase plasmid with $\alpha/Lk_0 = -0.027$ (17)]. There are two branch points, indicated by asterisks. Overcrossings and undercrossings are indistinguishable.

When superhelical DNA is examined microscopically, it is found to be essentially always plectonemically interwound, with some proportion of branched structures (17, 18). This interwound configuration, an example of which is shown in Figure 1, was said to be supercoiled because the winding involved was of a higher order than the duplex winding of the Watson-Crick helix itself. (The term superhelicity formally refers to the topological constraint, whereas supercoiling refers to the tertiary structures that are observed in superhelical molecules.)

When the DNA is coated with RecA, its effective thickness increases, allowing one to distinguish over-crossings from under-crossings. This allows one to determine the writhing numbers of these molecules. If they are taken from a

fully characterized population that is topologically identical (and hence all have the same superhelicity), one knows both Lk and α . So from Equation 1, one can infer Tw , which is otherwise difficult to measure directly.

Electron micrograph (EM) data can be used to assess population averages of a variety of parameters of DNA supercoils, including branch number, average supercoil diameter, and Wr . However, the relationship of these results to solution conformations is not clear. In preparing samples for the electron microscope, the DNA is adsorbed on a surface where it experiences large spreading forces, then it is dried and coated with metal. These drastic manipulations could make the resulting configurations unrepresentative of the shapes of the DNA when free in solution. Certainly the observed structures are not projections onto a plane of the solution structures, as they must preserve length. However, small angle X-ray scattering and cryoelectron microscopy, which probe solution structures, both also find interwound conformations (19, 20). So the interwound geometry itself is quite robust, although the parameter distributions found by analyzing populations of EM images may not be representative of the solution properties.

The Energetics of DNA Deformations

Investigations of DNA energetics proceeded in parallel with analyses of its structure. Because DNA was initially assumed to be linear, the first associations of energetics with deformations involved only bending deformations. These focused on assessing the thermal equilibrium behavior of long, unconstrained molecules subjected to random thermal motion. Twist was not considered because it was not regarded as relevant to this process. Once it was realized that DNA could be superhelical, so that twisting and bending were coupled by Equation 1, more complex models were introduced.

THE MECHANICS OF DNA AS A LINEAR POLYMER It was known early on that DNA is stiff, but not infinitely so; sufficiently long linear segments can be deformed into random coils by thermal motion. Previously developed methods of polymer physical chemistry were directly applied to analyze these large-scale deformations. Specifically, a linear DNA molecule was represented in various ways as a jointed chain, an idea that dates back at least to Kirkwood & Riseman (21).

The two major classes of such models are the Gaussian chain (or random-walk) and the wormlike coil. The Gaussian chain model divides the molecule into n uncorrelated segments of length l_r , such that the mean square end-to-end distance, $\langle R^2 \rangle$, is given by

$$\langle R^2 \rangle = nl_r^2. \quad (4)$$

The Kratky-Porod wormlike coil (22) is effectively a Gaussian chain taken in the limit $l_r \rightarrow 0$, i.e., so the molecule forms a continuous curve with

$$\langle R^2 \rangle = \frac{l_c}{\lambda} + \frac{1}{2\lambda^2} \{ \exp(-2\lambda l_c) - 1 \}. \quad (5)$$

Here, $l_c = nl_r$ is the molecular contour length, and $\frac{1}{\lambda}$ is the Kuhn statistical length. The persistence length $\frac{1}{2\lambda}$ is the minimum contour length needed for the initial tangent direction to be randomized by thermal fluctuations. Equivalently, it is the effective radius of the random coil produced by an arbitrarily long DNA. The value of the persistence length of DNA has been measured under a variety of conditions (23–25). As shown below, this view of DNA mechanics may be interpreted in terms of linear elasticity, but originally it was not described that way.

In 1958, Landau & Lifshitz (26) proposed an explicitly elastic model to analyze thermal fluctuations of linear molecules. The polymer was regarded as a threadlike elastic curve, with constant length and zero thickness, making it analogous to the Kratky-Porod wormlike coil. Its unstressed shape was regarded as straight, with energy required for bending. If the curvature at position s is $\kappa(s)$, then the free energy density needed to bend the DNA to that curvature is quadratic,

$$F(s) = F_0(s) + \frac{1}{2}A\kappa^2(s), \quad (6)$$

where $F_0(s)$ is the free energy density associated with the equilibrium (straight) conformation, and A is the bending stiffness. The bending energy is the integral of this density, and hence is an extensive conformational property. In this analysis, the mean square end-to-end distance is

$$\langle R^2 \rangle = 2 \left(\frac{A}{kT} \right)^2 \left\{ \frac{l_c kT}{A} - 1 + \exp(-l_c kT/A) \right\}, \quad (7)$$

where k is Boltzmann's constant and T the temperature. Comparison of Equations 5 and 7 gives the expression (27, 28)

$$A = \frac{kT}{2\lambda}, \quad (8)$$

which suggests that a persistence length is equivalent to an effective bending stiffness in a linear model.

Landau & Lifshitz explicitly described the bending energy in their model as a Helmholtz free energy. This was justified by the fact that molecules in their model, having no thickness, have effective volumes equivalent to their constant lengths. The Landau-Lifshitz approach has been extended to cases in which the system volume is not necessarily constant, but the temperature and pressure are assumed to be so, i.e., the bending energy in these cases is equated with a Gibbs free energy (28–30).

Gray & Hearst (28) first evaluated the enthalpic and entropic contributions to the free energy of bending. They showed that for a linearly elastic polymer that is bent to uniform curvature κ , a plot of $\frac{k}{4\lambda}$ versus $\frac{1}{T}$ will be linear, with slope corresponding to $\Delta H_i/\kappa^2 l$, the enthalpy of bending per unit curvature squared per unit length, and intercept corresponding to $\Delta S_i/\kappa^2 l$, the entropy of bending per unit curvature squared per unit length. Using a relation derived in Reference 23, Gray & Hearst estimated the Kuhn length as a function of temperature from

sedimentation data, and thereby evaluated the enthalpy and entropy of bending to be (28)

$$\frac{\Delta H_l}{\kappa^2 l} = 77 \pm 25 \frac{\text{kcal } \text{\AA}}{\text{radian}^2 \text{ mole}},$$

$$\frac{\Delta S_l}{\kappa^2 l} = -0.17 \pm 0.09 \frac{\text{kcal } \text{\AA}}{\text{radian}^2 \text{ mole K}}.$$

These authors point out that the negative entropy result, if it can be taken at face value in light of experimental uncertainties, has intriguing implications—for instance, the possibility that bending somehow orders ambient solvent. We note that a negative entropy also implies that the bending stiffness of DNA would increase with temperature. There is substantial experimental evidence (described below) that the entropy associated to DNA superhelicity (as distinct from bending) is in fact positive. We will return to this issue later.

THE FULL ELASTIC MODEL A superhelical DNA domain, whether a circular molecule or a loop within a longer region, is not able to deform so as to relieve its constraint. Moreover, as shown in Equation 1, the superhelical constraint couples bending deformations (involving writhe) with twisting deformations. So once it was understood that DNA occurs in superhelically constrained states, the need for a more complete treatment of its mechanics became clear.

In the first such analysis, the molecule was regarded as being linearly elastic, and hence endowed with a full set of elastic parameters—two bending stiffnesses A_1 and A_2 , and one torsional stiffness C (31). The unstressed state of the molecule was taken to be straight, with a helical twist rate of 10 base pairs per turn. If $\kappa_1(s)$ and $\kappa_2(s)$ are the curvatures in the principal directions as functions of position s , and $\tau(s)$ is the helical deformation density there, then in linear elasticity the energy associated with this conformation in a molecule of length L is

$$E = \frac{1}{2} \int_0^L A_1 \kappa_1^2(s) + A_2 \kappa_2^2(s) + C \tau^2(s) ds. \quad (9)$$

In the first analyses of this type, the DNA was regarded as a superhelically constrained circular molecule, with the mechanical properties of a homogeneous, isotropic, linearly elastic, mechanically symmetric (i.e., $A_1 = A_2$) rod (31–33). These assumptions embodied the simplest elastic properties and conformed to the then-current view that unstressed DNA had a uniform, straight, helical structure. As more precise information became available, it became clear that both the unstressed shape and the mechanical properties (i.e., elastic parameters) in fact could vary with base sequence. Moreover, more complex energy laws, including stretch and shear, and the possibility of terms coupling bending and twisting, were also considered. This work is described in the following sections.

The assumption of linear elasticity has a more precise justification. If DNA is a conservative system, it will have energies associated with deformations. One may

expand the local energy density in a Taylor series as a function of the generalized coordinates $\kappa_1(s)$, $\kappa_2(s)$, and $\tau(s)$, setting the zero point to correspond to the undeformed structure. Because the undeformed structure has minimum energy, the zeroth and first-order terms in the Taylor series vanish, so the lowest order terms are quadratic. The original linearly elastic model results when one only considers these terms, and there are no cross terms. Although the deformation energies may in fact also have higher order terms, which would make DNA nonlinearly elastic, their evaluation would require measuring higher order effects.

EXPERIMENTAL MEASUREMENTS OF DNA MECHANICAL PARAMETERS An effective bending stiffness was inferred from the measured persistence length of DNA, as shown in Equation 8 above, from which the value $\frac{1}{2\lambda} = 50$ nm for DNA under physiological conditions yields $A \sim 2.0 \times 10^{-19}$ erg cm. If DNA is in fact linearly elastic, homogeneous, and symmetric, then this would be its actual bending stiffness. If there is asymmetry, so $A_1 \neq A_2$, the effective bending stiffness would be the harmonic mean of these two stiffnesses.

When DNA crystal structures became available, it was immediately clear that the actual structure of the molecule varies somewhat with base identity and near neighbors. One could surmise that other parameters, including those describing the mechanical properties, may also be sequence dependent. Unfortunately, many of the methods available to measure bending or torsional stiffnesses of DNA yield averages over substantial lengths (the persistence length, in the analysis leading to Equation 8). Although one can infer a sequence effect if experimental results for AT-rich and GC-rich DNA differ, it is difficult to determine the precise sequence specificity of the stiffnesses from such experiments.

An effective torsional stiffness was first measured by Barkley & Zimm using fluorescence depolarization (34). Here a fluorescent dye is intercalated into the DNA, and the molecule is illuminated with polarized light at a wavelength absorbed by the dye. Any change in the orientation of the dye between absorption and fluorescent emission is observed as a depolarization. The extent of this depolarization can be used to estimate a torsional stiffness. This method assumes that the dye's motion is a faithful reflection of the torsional fluctuations the DNA would experience in the absence of the dye. And the value measured is the average over all sequence positions at which intercalation occurs.

This procedure found torsional fluctuations of 5 to 7 degrees between neighbor base pairs, which showed DNA to be a remarkably flexible molecule. Rather than having a well-specified interpair helical twist of approximately 34 degrees, at room temperature the actual value fluctuates between 28 and 40 degrees, and one third of the time it undergoes excursions beyond those limits. Fluctuations of this magnitude are occurring simultaneously for all base pairs. Clearly, the rigid picture of DNA structure resulting from X-ray crystallography is an artifact of that method. The actual molecule is vastly more flexible.

A second method to measure the DNA torsional stiffness uses ring closure probabilities (35, 36). Here a short, nicked circular DNA molecule containing a

known number N of base pairs is constructed. N is chosen so the unstressed twist of the molecule is not integral. Then a ligase enzyme is introduced. This closes the nicks, producing closed circular molecules having integer linking numbers. Because closure requires torsional fluctuations that either overtwist the molecule to the next higher (integer) value of Lk or undertwist it to the next lower value, the ratio between these two topoisomers in the resulting population will depend on the effective torsional stiffness. (By using short molecules bending effects are excluded.) A succession of molecules is generated, each of which is one base pair longer than its predecessor, and the fraction of molecules with each linking number is measured for each length N . The results permit the evaluation of a sequence average torsional stiffness C of the DNA. Values of C from this procedure range from 300–400 pN nm².

More recently, mechanical parameters have been obtained from micromanipulation experiments in which the ends of single DNA molecules are attached to micron-scale beads held with magnetic or optical “tweezers” or micropipettes. This arrangement allows individual DNA molecules to be stretched, twisted, subjected to magnetic fields, or immersed in hydrodynamic flows. Force and extension measurements, and comparisons of bead motions with expected magnetic or hydrodynamic behavior, permit assessment of a wide range of properties, such as bending, torsional and entropic elasticity, and characterization of both responses to enzyme action and transitions to unusual forms induced by extreme stresses (37–41). For example, Bryant et al. (42) have directly measured a DNA torsional stiffness by observing the rotation of calibrated “rotor” beads attached to twisted and stretched molecules near a site-specific nick. They measured a stiffness of $C = 410 \pm 30$ pN nm², 40% to 50% higher than that obtained from topoisomer distribution experiments. The authors note that this discrepancy may be due either to the high tension imposed on the molecules in their experiments or an inability of previous experiments to adequately constrain writhing degrees of freedom. This illustrates the fact that because single-molecule micromanipulation assays are not likely to sample the same ensembles of structures explored by molecules in their *in vivo* environments or in solution, mechanical or thermodynamic parameters obtained from these studies are not necessarily directly applicable to physiological DNA.

The only method that explicitly derives sequence-dependent mechanical properties involves the analysis of the deformations of DNA structure in cocrystals with protein molecules (43). This approach provides information on deformability at the atomic level, which is considerably more detailed than what is possible using other approaches. However, it assumes that the deformations imposed on DNA by binding proteins are a faithful reflection of the deformations the molecule would undergo if it were free in solution.

THE ENERGETICS OF SUPERHELICITY The free energy associated with DNA superhelicity was first measured by Bauer & Vinograd using dye intercalation

(44). Because the intercalation of a dye molecule between neighbor base pairs decreases the twist angle between the pairs, in a negatively superhelical domain it “captures” a portion of the linking difference at the intercalation site, which causes the rest of the domain to relax by a corresponding amount. This relaxation decreases the unfavorable free energy associated to superhelicity, which drives the binding equilibrium toward the bound state. Conversely, when the DNA is positively superhelical, the unwinding caused by dye intercalation increases the superhelical stresses in the domain. The increment of superhelical free energy required will diminish the binding equilibrium below the level seen in an unconstrained linear molecule. By measuring the binding equilibrium with different amounts of added dye, hence different amounts of either induced relaxation or stress, one can determine the extent to which the resulting changes of effective superhelicity assist or impede binding. In this way Bauer & Vinograd (44) measured the free energy associated with superhelicity over a wide range of both positive and negative linking differences.

If sufficient nicks are introduced into circular DNA molecules their linking numbers can change. If this process comes to equilibrium it will generate a population distributed around the relaxed state (16, 45). These topoisomer distributions have been shown to be effectively Boltzmann (i.e., Gaussian), although once closed the molecules only take on integer values. The mean of this distribution gives the linking number of the relaxed state, and from the variance one can determine the free energy of superhelicity. This procedure, called the Gaussian centers method, only evaluates the free energy around the relaxed state.

Sufficient negative DNA superhelicity can drive local transitions to other secondary structures whose right-handed helicities are smaller than that of the B-form helix. If the energetics of the transition involved are well understood in linear molecules, a quantitative analysis of the extent of transition in a range of topoisomers allows one to evaluate the free energy associated to superhelicity (46). This procedure evaluates the free energy of superhelicity around the stress levels that drive transitions, which usually occur at substantially negative linking differences. As topoisomer transition data can be gathered at different temperatures, this procedure has been used to evaluate the temperature dependence of the free energy of superhelicity.

The first two methods find the free energy of superhelicity to be essentially quadratic in the linking difference α , with a coefficient that is inversely proportional to molecular length:

$$\Delta G(\alpha) = \frac{qRT}{N}\alpha^2. \quad (10)$$

(The dye binding method, which is the only one that maps out the free energy over large ranges of α , also suggested the possibility of a very small asymmetry.) The transition competition method assumes a quadratic functional form, and evaluates its coefficient. At the time Bauer & Vinograd performed their dye-binding

experiments, the dye used was thought to untwist DNA by 12° per intercalation event. A subsequent reevaluation found it actually untwists by 26° per event. Once this correction has been made, all three methods evaluate the quadratic coefficient to be near $q \approx 1110$.

The transition competition method has been used to evaluate the free energy of superhelicity at a variety of temperatures (46). This enabled $\Delta G(\alpha)$ to be decomposed into its enthalpic (ΔH) and entropic (ΔS) contributions as

$$\Delta G(\alpha) = \Delta H(\alpha) - T\Delta S(\alpha). \quad (11)$$

The values found under the experimental conditions of Bauer & Benham (46) are $\Delta H(\alpha) = 1893\alpha^2/N$ and $\Delta S(\alpha) = 3.735\alpha^2/N$. The conclusion that $\Delta S(\alpha)$ and $\Delta G(\alpha)$ are both positive at room temperature means that the enthalpy of superhelicity exceeds its free energy, and that this free energy decreases as temperature increases. These conclusions are supported by multiple other lines of evidence. Lee et al. (47) used van't Hoff methods to measure the enthalpy of superhelicity, $\Delta H(\alpha)$, whereas Seidl & Hinz (48) used microcalorimetry for the same purpose. Both groups found that this enthalpy substantially exceeds the free energy $\Delta G(\alpha)$ at room temperature, which requires a positive entropy. Duguet (49) evaluated the temperature dependence of the free energy of superhelicity using the Gaussian centers method. He also found that this free energy varies essentially linearly with T , with a negative slope indicating again that $\Delta S(\alpha) > 0$.

So all available experimental data indicate that the entropy of superhelicity is large and positive. This contrasts with the negative entropy of DNA bending found by Gray & Hearst (28). It also stands in opposition to the entropy values derived from theoretical analyses of the large-scale structure of superhelical DNA, as is described below. These uniformly find a negative entropy, consistent with the increasingly constrained set of interwound tertiary structures available to incrementally superhelical molecules.

METHODS TO ANALYZE THE STRUCTURE OF SUPERHELICAL DNA

There are three qualitatively different approaches to the analysis of the structure of superhelically constrained DNA. In all cases, one regards the DNA as having an unstressed conformation, deformations away from which require energy. At increasing levels of refinement, these attributes can be regarded as sequence dependent. The first method proposed for analyzing superhelical DNA sought the mechanical equilibrium configuration, which is the minimum energy configuration of the topologically constrained molecule (31–33). This has the advantage of being a relatively tractable problem. However, mechanical equilibria may not be fully representative of the actual behavior of superhelical DNA. At finite temperatures, random thermal motion drives molecules into higher energy configurations.

So equilibrium in this case is a distribution among all available states, with high energy states exponentially less occupied than low energy states. The second class of methods uses statistical mechanics to analyze superhelical DNA structure by either calculating or simulating this distribution. In this view, the mechanical equilibrium configuration corresponds to the structure the molecule would have at $T = 0$ K. These methods elucidate the behaviors of populations of molecules at equilibrium at ambient temperatures; however, they do not say anything about the dynamics of deformations in DNA or the rates at which individual molecules move among the states. Further, both of these approaches calculate equilibria. If the DNA is not at equilibrium their results may not be useful. For this reason, dynamic methods also have been developed. Here we briefly describe each approach.

Mechanical Equilibrium Methods

These methods calculate the minimum energy configuration of a topologically constrained circular DNA molecule, the constraint being the constancy of its linking number. Mathematically, a set of local coordinates is embedded in the polymer at each position s along its central axis. The shape of the molecule at mechanical equilibrium is calculated by finding the orientations of these local coordinates with respect to a fixed set of lab coordinates, as functions of s .

The first approach, based on Kirchhoff rod theory, modeled the DNA as a homogeneous, isotropic, linearly elastic rod that is straight when unstressed (31–33, 50, 51). It also assumed no external forces or torques were imposed on the molecule. This method formally calculates the shape of the elastica curve, which is the central axis curve of the rod. Only deformations of curvature and of twist were permitted. Under these conditions it was shown that the mechanical equilibria were toroidal helices. The stability of these equilibria initially was not assessed.

This approach has been extended and refined in a variety of ways. The system of local coordinates and the parametrization of the coordinate transformation can be chosen in different ways to suit specific purposes. The first approach used the mechanically determined principal axes of each cross-section, and described the coordinate transformation using Euler angles. However, the Euler angle transformation has an inherent singularity that can be removed by using instead Euler parameters. Other approaches based on differential geometry use the Frenet frame as local coordinates and the curvature and torsion as transformations. Shi et al. (52) showed that use of cylindrical local coordinates enabled closed-form solutions to be found, even in a considerably more general formulation.

Elastic equilibrium analyses using more detailed models of DNA have been presented. Sequence dependence of the unstressed DNA structure has been included (53). A recent extension also incorporates sequence dependence of the deformation energies, as estimated from crystal structure data (54). An elastic rod model in which the DNA is regarded as explicitly double helical also has been introduced

(55). The set of allowable deformations has been expanded to include shear and extension, in addition to twist and bending (52). This has the important practical effect of allowing more highly deformed states to be analyzed than are possible with elastica-based theories, where the curvature must be so gradual that the finite diameter of the rod, and hence shear effects, can be ignored.

Regarding stability, LeBret showed that, in the initial elastica theory, as the superhelicity decreased away from zero the mechanical equilibrium initially remained a planar circle, with all the deformation partitioned to twist (56). However, as the deformation was continued a bifurcation occurred to writhed conformations (57). This behavior had been independently discovered in analyzing hocking of submarine cables (58). A finite element analysis has shown that this bifurcation behavior is stringently dependent on the precise unstressed shape of the elastic rod (59). If there is a single kink in an otherwise straight rod, the bifurcation occurs earlier, while the presence of two kinks can lead to different twisting behaviors in the two regions of the circle they bound. Interestingly, if the DNA is regarded as naturally curved, forming an O-ring when unstressed, the bifurcation to writhing does not occur. Instead, the molecule immediately deforms to a writhed state as soon as any linking difference is imposed. Maddocks and coworkers have made an exhaustive bifurcation analysis of the equilibrium configurations available to a superhelical DNA, as a function of α (60, 61). They assume the molecule can pass through itself, so self-contacts do not occur. They again find large families of mechanical equilibrium structures as mechanical and bifurcation parameters are varied. All are approximately toroidal helical structures.

When superhelical circular DNA is examined microscopically, it is found to be essentially always plectonemically interwound, with some proportion of branched structures (17, 18). Small-angle X-ray scattering and cryoelectron microscopy, which probe the solution structure, also find interwound conformations (19, 20). This leads to an apparent discrepancy between the observed structures and the predictions of mechanical equilibrium analyses.

This problem is resolved when one notes that the models used to calculate mechanical equilibria assume no externally imposed forces or torques on the DNA. When the molecule comes into self-contact, each side of the contact point exerts a force on the other, so the assumption of no external forces implicitly excludes self-contacts. The precise conclusion of these analyses is that, in the absence of self-contacts, the only equilibria are toroidal. Because superhelical DNA in fact is interwound, not toroidal, it follows that these so-called plectonemic structures are stabilized by the forces of self-contact that they experience. In their absence, interwound structures would not be equilibria.

Several groups have extended the mechanical approach to include forces of self-contact. This was done initially using finite element methods (62). Later, contact forces were successfully incorporated into a rigorous analysis of the elastic stability of superhelical DNA configurations (63, 64). These analyses show that in

the presence of self-contacts, the equilibria are indeed interwound. This conclusion has important implications, which are presented below.

Statistical Mechanical Methods

At finite temperatures, random thermal motion will cause a molecule to sample states whose energies are above the absolute minimum. So the equilibria that occur are statistical distributions in which a population of identical molecules samples all possible states, with the relative frequencies of two states varying exponentially with their energy difference. In practice, one must make drastic simplifying assumptions before either this approach or the dynamics approaches, examined below, become tractable. Even if one assumes the molecule has no cross-section, but instead is a mathematical closed curve with smoothly varying curvature and helicity, the problem remains intractable, for several reasons.

First, because the curvature and twist are specified at each point, the state space is infinite dimensional. One cannot allow curvature to vary arbitrarily because the molecule must remain topologically closed circular. It is an unsolved problem of differential geometry to determine which curvature and torsion functions are consistent with smooth closure, so the configuration space of allowable curvature functions is not known.

Second, although the twisting energies and constraints are harmonious, those relevant to bending have fundamentally different characters. Specifically, the total twist Tw is an extensive parameter, found by integrating the twist density $\tau(s)$ as shown in Equation 3. The energy of twisting is also extensive, given in the linear elastic case by integrating an expression in the same intensive parameter τ (see the twist part of the integral in Equation 9). In contrast, the conformational constraint relevant to bending deformations is the writhing number Wr . Being an inherently interactive parameter, given by a Gaussian double integral, it bears no simple relationship to any intensive parameter, such as the curvature $\kappa(s)$. Yet the bending energy, which is the energy associated to changes of tertiary structure, is an extensive parameter of the intensive curvature. So the writhing constraint on tertiary structure and the energy density associated to deformations of tertiary structure have fundamentally different characters.

For these reasons, calculations of structures and energetics are not tractable for conformations of superhelically constrained DNA molecules having smoothly varying curvatures and twists, other than the mechanical equilibria. So various simplifications are required, which we describe in sequence. First, in both statistical and dynamic models, the infinite dimensionality of the state space is resolved by assuming the molecule consists of a finite number of straight segments joined by flexible joints of some type. Energy of bending is then associated to the angles between neighbor joints. As there are a finite number of joints, the state space for bending is now finite dimensional. There are a variety of such models.

The crudest is a statistical segment model in which the length of each segment is the Kuhn segment length and the joints are universal joints, so there is no energy associated to the intersegment angles. To understand the limited relevance of this class of models, note that a sufficiently long, linearly elastic polymer under random thermal buffeting will assume a random coil conformation whose effective diameter equals the Kuhn segment length. A few moments of drawing random coils with pencils, then trying to approximate them with a set of statistical segments of equal total length, each the diameter of the coil, will convince one of the inability of such models to accurately represent conformations of continuously varying polymers. Calculation of Wr is particularly problematic. Because neighbor segments do not cross in projection, they make no contribution to Wr . So, in this model, points can only contribute to Wr if they are more than approximately three persistence lengths (i.e., 150 nm) apart! One anticipates that this would lead to a substantial underestimate of the writhe of a smoothly varying molecule.

One can also approximate the smooth curve of an elastic polymer by a sequence of shorter segments, with a quadratic energy associated to bending the intersegment angle away from straight. By varying the segment length and number so the total length is fixed, and also varying the bending stiffness (i.e., the coefficient of the quadratic) in synchrony, one can model with successively better refinement—even taking it to the continuum limit. The hydrodynamic properties of linear, flexible polymers can be approximated by assuming the segments are in fact beads.

In these segment-based models of superhelical DNA, the discordance between parameter types is handled as follows: The writhing number of each configuration is calculated first. This is subtracted from the assumed linking difference, and the difference is ascribed to twist. In the early models this twist was assumed to be uniformly distributed, and the quadratic energy associated with it was calculated. This approach allows bending to fluctuate, but twist must instantly equilibrate without fluctuations. This effectively allows bending to occur at finite temperature, but constrains twisting to $T = 0$ K. Recent approaches have corrected this simplification (65–67).

Jointed chain, bead, or continuum models can be used to calculate attributes of equilibrium distributions for linearly elastic polymers with free ends (22, 23, 27, 68–70). However, these methods encounter substantial difficulties when the molecule is topologically constrained. So investigators instead use Monte Carlo methods (71, 72), which sample the thermal equilibrium distribution instead of calculating it exactly.

The basic Monte Carlo strategy involves two steps. One starts the molecule in a current state C whose energy is E_C . Then one selects a new state N having energy E_N . Finally, one determines whether to stay in the current state or move to the new state. This is done iteratively, and a distribution is built by periodically sampling the current state.

Two conditions must be met for this procedure to converge to the equilibrium distribution. First, the state selection step must not introduce any bias. This requires that it satisfy two subconditions, ergodicity and detailed balance. Ergodicity

requires that every state can be reached from any current state, either directly or by a finite sequence of steps. That is, if one constructs a directed graph of all allowable choices of new state that can be made, for all initial states, ergodicity requires the result to be a connected digraph with every point accessible from any other point by a path consisting of directed edges. Detailed balance requires that the process of selecting the new state be unbiased. Specifically, let $p(N|C)$ be the probability of selecting new state N , given one is in current state C . Then detailed balance requires that, for all states A and B , $p(A|B) = p(B|A)$. Satisfying detailed balance can be surprisingly difficult, as is shown below. The second requirement for faithfully sampling an equilibrium distribution is that once the new state N has been chosen, the decision whether to stay in C or move to N must be consistent with equilibrium statistics. The following Metropolis criterion is most commonly used. If $E_n < E_c$, move to the new state N . Otherwise, choose a random number r uniformly distributed on the closed interval $[0, 1]$. If $r < \exp(-(E_n - E_c)/RT)$, move to N ; otherwise, stay in C . In their classic paper, Metropolis et al. (73) showed that if the selection step satisfies ergodicity and detailed balance, and if the Metropolis decision criterion is used, then the distribution generated will asymptotically converge to the equilibrium distribution.

Unfortunately, in practice the rate of convergence of this method can be difficult to determine, and is often exceedingly slow. In that case, several remedial steps can be taken to decrease the correlations between successively sampled states. One can build one's distribution by performing multiple iterations of the above two-step process before selecting the next sample state. If this does not suffice, supplementary selection steps can be introduced that are designed to more rapidly move through the configuration space. However, these also must satisfy ergodicity and detailed balance.

The condition of detailed balance can be especially difficult to satisfy. For example, suppose that in current state C there are n_c possible choices of new state, each of which may be selected with equal probability, $1/n_c$. Although this would seem a safe criterion, in fact it will violate detailed balance unless every state has the same number of possible choices. To see this, consider the state space in Figure 2, in which four states are denoted by vertices A, B, C, and D, and the possible choices of new state are shown as edges between pairs of vertices. Note that vertices B and C have three connections, whereas vertices A and D have only two. If one is currently in state A, there are two choices of new state. If one chooses either at random, the probability of choosing state B is $p(B|A) = 1/2$. But if one is in state B there are three possible choices of new state. If one again chooses at random from among them, then $p(A|B) = 1/3 \neq p(B|A)$. So this simple and seemingly fair criterion actually violates detailed balance unless all states have the same number of possibilities. From this example one sees that satisfying detailed balance can require a careful analysis of the connectivities within the entire state space.

The most extensive application of the Metropolis Monte Carlo method to the analysis of superhelical DNA has been made by Vologodskii et al. (72), who model the molecule as a chain of segments that is closed into a topological circle.

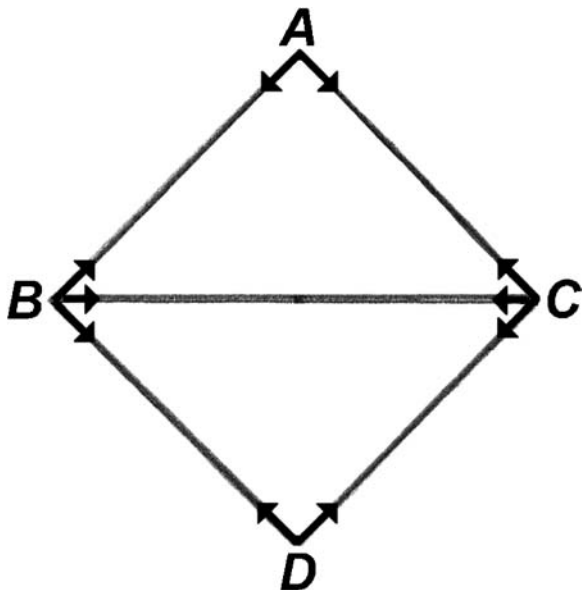


Figure 2 State space illustrating violation of detailed balance. The probability of moving from state A to state B is $\frac{1}{2}$, but the probability of moving from B to A is $\frac{1}{3}$.

A quadratic bending energy is associated with deviations from straightness of each angle between successive segments, and the $T = 0$ K approximation for twist energy is made, as described above. Two types of trial motions are used to select the new state from the current one, as shown in Figure 3. In the crankshaft move (Figure 3A) two vertices are selected at random, and the subchain they bound is rotated through angle ϕ around the axis joining them. Here ϕ is chosen at random, uniformly distributed in the interval $0 \leq \phi < 2\pi$. As this move can result in strand crossings, it has the potential to change the topological type of the molecule. As long as this is regarded as allowable, this crankshaft move will satisfy detailed balance but may not conserve topology. If topology is to be conserved, then some rotation angles may be forbidden for specific pairs of vertices. Care must be taken in the design of this move to assure it does not violate detailed balance.

The second trial motion is reptation, in which two disjoint subsections of the chain are exchanged as shown in Figure 3B. Here one chooses two vertices at random (e.g., V_1 and V_2 in the figure), and selects for exchange the disjoint subchains they bound. The lengths of these subchains can also be chosen at random, confining oneself to small values. In Figure 3B, the 3-subchain bounded by $[V_1 - 3, V_1]$ is to be exchanged with the 4-subchain bounded by $[V_2, V_2 + 4]$. Once the subchains to be exchanged are identified, the interior angles of each are uniformly either increased or decreased so they span the gap to which they will be moved. Only

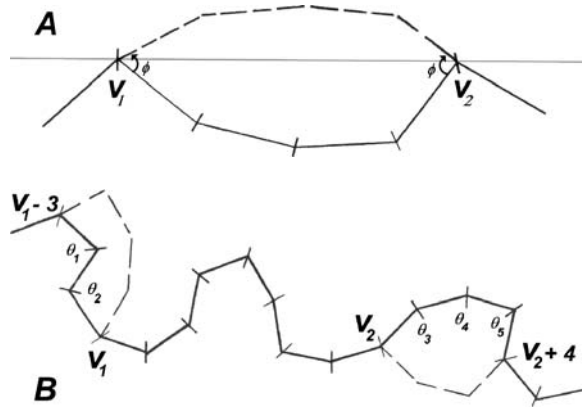


Figure 3 Trial motions employed in the Monte Carlo method of Vologodskii et al. (adapted from Reference 72). *A.* Crankshaft move. A section of the chain is rotated through a random angle, ϕ , about an axis connecting two randomly chosen vertices, v_1 and v_2 . The new configuration of the affected segments is represented by a dashed line. *B.* Reptation move. The angles θ_1 – θ_5 are modified so that the two randomly chosen sections of the chain bounded by $[v_1 - 3, v_1]$ and $[v_2, v_2 + 4]$ can be exchanged. Again the alteration is represented by dashes.

pairs of subchains in which each member can fit into the gap left by the other can be exchanged. Starting in any state, one chooses the pairs of subchains to be exchanged randomly and with equal probability from among all possibilities.

If any subchain could be moved to any other position, reptation (if carefully implemented) would satisfy detailed balance because every state would have the same number of possible choices. Because this is not the case, this reptation move violates detailed balance. To see this, consider the two states shown in Figure 4, where a 4-chain is exchanged with a 3-chain. The essence of the problem is that not all 4-chains may be possible choices. If the gap created by removing a 4-chain is greater than $3L$ (L is the length of a segment) then no 3-chain can span it. So the possible choices are only those 4-chains whose end-to-end distances do not exceed $3L$, the number of which can vary from one state to another. In state *A* of Figure 4 there is exactly one 4-chain whose gap is small enough to be spanned by a 3-chain. If there are N segments in this molecule, then there are $N - 6$ choices of 3-chain, and one 4-chain, that can be exchanged. If each choice has equal probability of selection, then $p(B|A) = 1/(N - 6)$, where state *B* is shown in the figure. In state *B*, however, there are four different choices of 4-chain whose ends are close enough to be spanned by a 3-chain, and for each of these there are $N - 6$ different 3-chains that could be selected. So if each choice has equal probability then $p(A|B) = 1/[4(N - 6)]$. As $p(A|B) \neq p(B|A)$, this reptation move violates detailed balance. Therefore, this implementation of the Monte Carlo method cannot be regarded as converging to the equilibrium distribution.

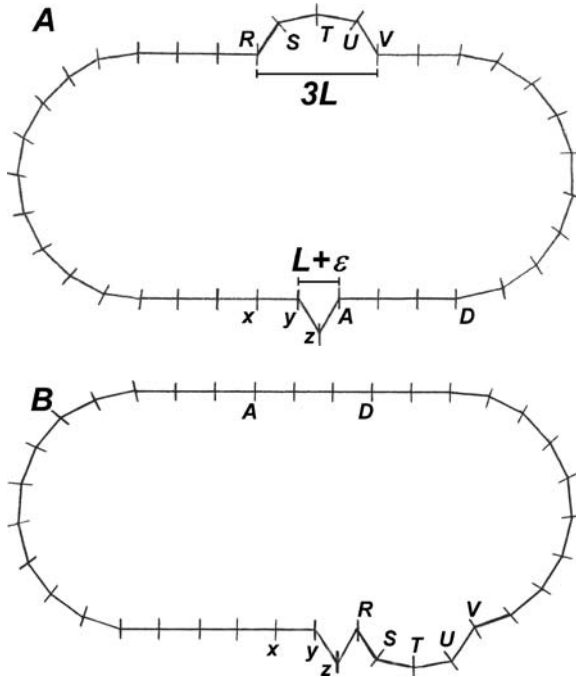


Figure 4 Reptation move violates detailed balance. In state *A*, there is one possible choice of 4-segment, *RSTUV*, whose ends are separated by $3L$. In this state there are $(N - 6)$ choices of 3-segment. Choosing segment *AD* and performing the reptation move produces state *B*, in which there are four possible choices of 4-segment for exchange with *AD*; if *RSTUV* is half a regular octagon, then $\overline{xS} < 3L$, $\overline{yT} < 3L$, $\overline{zU} < 3L$, and $\overline{RV} = 3L$, so any of these could be chosen. Hence, in this state there are $4(N - 6)$ ways to perform the reptation move, and $\frac{1}{N-6} = P_{AB} \neq P_{BA} = \frac{1}{4(N-6)}$.

Vologodskii et al. (72) found that the crankshaft move alone generated a smaller fraction of branched supercoiled structures than what was observed experimentally. So they introduced the reptation move to raise the frequency of branching to that seen in electron micrographs (EM). But EM sample preparation requires the DNA to be spread on a planar grid, which may cause the conformational characteristics of a population, and in particular its branching frequency, to differ from those achieved in solution. So it is not clear that EM provides the best experimental comparisons for these purposes. CryoEM, which does not suffer this disadvantage, may prove to be better suited.

APPLICATIONS TO THE ANALYSIS OF SUPERHELICAL DNA Statistical methods, if they faithfully reflect the equilibrium distribution, enable comparisons to be made with experimental information on the conformational properties of populations of

molecules. They also have been used to assess the configurational entropy associated with supercoiling, as well as other energetic and thermodynamic quantities.

Hearst & Hunt (74) have applied a wormlike coil method to estimate the distribution properties of highly supercoiled DNA. They restrict consideration to simple plectonemes, which are interwound supercoils without branches. With this restriction they find that the molecule persists in a highly restricted condition in which its configurational entropy is greatly reduced. This suggests that the molecule may not wander far from its mechanical equilibrium configuration. If correct, this indicates that the results of mechanical equilibrium calculations may provide reasonable approximations of the conformational attributes of DNA at finite temperatures.

The Monte Carlo method of Vologodskii et al. (72) has been applied to evaluate by simulation a wide variety of conformational, energetic, thermodynamic, and/or hydrodynamic properties of superhelical DNA. Despite the formal problem this method has with satisfying detailed balance, its accuracy in evaluating conformational parameters (superhelix geometry, axis length, writhe, even knot-type frequencies) has generally been reasonably good. However, it has been less successful at assessing the thermodynamic parameters associated with DNA superhelicity. In particular, all statistical analyses of superhelical DNA performed to date find a negative entropy, consistent with the constraints imposed by plectonemic interwinding. The enthalpy of superhelicity, which has sometimes been identified with the elastic energy (72, 75), is calculated to be less than its free energy. These results strongly conflict with all experimental data, which measure a large enthalpy and a large positive entropy associated with superhelicity. If the entropy of superhelicity were negative, the free energy of supercoiling would increase with increasing temperature; the molecule would become stiffer. The opposite behavior is seen in practice. This discrepancy suggests that the large-scale configurational properties of supercoils, as found by these strictly elastomechanical models, do not dominate their energetics. Instead, superhelically driven changes in smaller scale attributes of molecular structure, such as the interactions between the DNA and the solvent, may play significant, even dominant, roles in determining the thermodynamics of this phenomenon.

Dynamic Methods

Dynamic methods calculate deterministic, time-dependent trajectories of the helix axes of individual DNA molecules by either numerical or analytical integration of the equations of motion. If this can be done over sufficiently long times, which are well beyond the scope of currently available methods, an individual molecule will sample its accessible states with a distribution that asymptotically converges to the equilibrium distribution of a population. Dynamic methods, like every other method that includes the possibility of self-contacts, find that superhelical DNA assumes interwound supercoiled configurations.

Numerical methods for simulating dynamic fluctuations in superhelical DNA have been widely implemented. In this section, we summarize several of the

principle approaches that have been taken. To date, these methods have been employed predominantly to simulate “equilibrium” dynamics in which closed, initially circular structures with specified linking differences, constrained by Equation 1, collapse to more stable interwound forms. More recently, fully dynamic, nonequilibrium scenarios have been explored. In such scenarios, which are likely more representative of *in vivo* events that involve DNA supercoiling, ΔLk itself varies dynamically in response to external processes, such as torsional loads imposed by bound proteins.

B-SPLINE LANGEVIN DYNAMICS Among the first dynamic models of DNA supercoiling was the *B*-spline representation of Schlick & Olson (76–79). In this method, the axis curve of ccDNA of length up to a few thousand basepairs is represented as a *B*-spline “ribbon” defined by a set of control vertices. The ribbon is characterized by linearly elastic energies of twisting and bending, as well as energies associated with self-contact, translational and rotational degrees of freedom, and restraint of the total contour length. As discussed above, the twist is assumed to remain uniformly distributed at all times. The work reported in References 78, 79 additionally includes salt-screened electrostatics via a Debye-Hückel term in the energy function. Deterministic trajectories of the vertices, and thereby also of the *B*-spline helix axis curve they generate, are obtained by numerically integrating the Langevin equations of motion (80) using an implicit-Euler algorithm (81).

This framework permits time steps larger than those available to traditional molecular dynamics (MD) schemes (100 femtosecond steps are taken in the simulations reported in References 76, 77), but requires setting γ , the “collision frequency” characterizing molecular damping and stochastic forcing owing to coupling with the heat bath, in a manner that freezes high frequency vibrational modes. This obscures the connection between numerical and physical times, leading to simulated motions estimated to be at least three orders of magnitude faster than “real” motions; simulations spanning nanoseconds in numerical time are proposed to correspond to dynamics occurring in microseconds of physical time (77). (The effect of varying γ upon supercoiling dynamics within this framework is fully explored in Reference 79.) This method has been used as described above to obtain energy-minimized conformations and to simulate equilibrium dynamics. As in the Monte Carlo work described previously, the generated structures were compared with electron microscopy data, with which they were deemed to be consistent. Results reported in Reference 78, which investigates the effects of salt concentration upon folding pathways, suggest that tightly interwound conformations are favored at *in vivo* and higher ionic strengths. This conclusion is in qualitative agreement with experimental results (19), but conflicts with predictions of statistical methods, which, as discussed above, account only for configurational contributions to the entropy.

This approach applies the equations of motion explicitly only to the finite set of vertices, then constructs the full molecular axis curve at each time step by *B*-spline interpolation from the vertex positions. This procedure need not conserve

topology. (An example of this behavior is shown in Reference 77, where a trefoil knot arises from an initial planar circle.) Any procedure involving calculations at a finite set of node points and interpolation of a curve will be guaranteed to conserve topology only if explicit tests for self-crossings are made at each time step.

DISCRETE-CHAIN BROWNIAN DYNAMICS In part as an effort to provide a model in which twist evolves dynamically, and simulation times correspond more closely with physical times, Chirico & Langowski introduced a discrete-chain Brownian dynamics (BD) procedure (65) based on a method originally developed for free linear DNA (82). In this method, the helix axis is represented as a segmented chain (a polygon in the case of ccDNA), whose vertices interact through linearly elastic twisting, stretching, and bending potentials. Twist-bend coupling, which allows the model to capture the effects of superhelicity upon the dynamics, enters through a set of torsional forces that result from the independence of the infinitesimal coordinates describing the axis (65, 83). For purposes of modeling collisions of the chain with solvent molecules (i.e., coupling with the heat bath), hydrodynamic beads are attached to the vertices, whose positions and relative twist angles are time-evolved using a second-order BD algorithm (84) that permits time steps as long as a few nanoseconds, and simulations out to milliseconds. [BD algorithms arise from numerical integration of the Langevin equations of motion in the overdamped regime (80).] The size of the beads is set according to the hydrodynamic diameter of B-DNA [e.g., the value 31.84 Å (85) is used in Reference 65], so that each bead represents several basepairs. Interactions resulting from local disturbance of the solvent owing to nonlocal motion of the chain (hydrodynamic interactions) are incorporated through a diffusion tensor (86). Contact (excluded volume) forces to prevent self-crossing of the chain are typically introduced either through Lennard-Jones potentials or Debye-Hückel electrostatics (87), which attempt to account collectively for backbone charges, excluded volume, and physiological ionic conditions. Like the *B*-spline approach, this framework has in general been used to simulate the folding of kilobase-length, closed (initially) circular structures of fixed linking differences into more stable interwound forms. Theoretical diffusion coefficient calculations by Langowski and coworkers based on their simulation results compare reasonably well with measurements obtained from dynamic light scattering experiments.

Extensions of this work (e.g., References 88–90) have investigated the effects of static bends, DNA-protein interactions, and external loads (see below) upon supercoiling dynamics. Because it assumes motions to be overdamped as a starting point, this method fails to resolve dynamics on timescales smaller than a few picoseconds.

DISCRETIZED CONTINUUM DYNAMICS Several numerical procedures for equilibrium dynamics based on Kirchhoff's elastic rod model have also been proposed. In one approach, the continuous axis curve of the rod is discretized into a number of points, with twists associated to those points. The dynamics of this model are

evaluated by numerically integrating a system of equations consisting of Kirchhoff's equations of motion, the constitutive relation of linear elasticity, and equations for the time evolution of twist (66, 91, 92). This approach typically includes self-contact through a stiff inverse power law potential centered at the discretization points. Viscosity is considered through a damping term. Stochastic forcing, either through a Langevin or BD formulation, is generally not considered because accurately correlating the thermal noise requires discretization approaching base-pair resolution. This would eliminate the numerical advantages of approximating the system as continuous in the first place (93), and calls into question the validity of that approximation at a scale on which the system might better be considered discrete. This may represent an advantage of discrete over discretized continuous approaches to dynamic modeling. Although the latter are computationally advantageous for simulations involving deformations of very large systems over long times, because thermal fluctuations certainly influence dynamics *in vivo*, the former may provide the best compromise between the coarse-graining necessary to model large-scale, long-time conformational changes, and the resolution necessary to account for both the finite temperature environment and the localized DNA features, like bending anisotropy, that contribute to those changes. In point of fact, Klapper & Qian have shown that the energy functionals characterizing these two approaches are fundamentally inconsistent with one another, an artifact of localizing twist and bend energy in the discrete case, and distributing it in the continuum case (93). The implications of this inconsistency remain unresolved.

VARIATIONAL (HAMILTONIAN) DYNAMICS The fully general form of the Hamiltonian/Euler parameter formulation of Maddocks and coworkers, discussed above in the context of static equilibrium and bifurcation analyses, provides equations of motion for the dynamics of both constrained (inextensible and/or unsharable) and unconstrained Cosserat rods. In a dynamic context, this formulation has the advantages (67) of being first-order in time, and relying upon continuous symmetries to generate integrals of the motion via Noether's theorem. On the other hand, as with discretized Kirchhoff rod approaches, although the Hamiltonian approach is capable of including self-interaction forces and obtaining interwound geometries, the facility and accuracy with which it is able to model the effects of an electrolytic environment at physiological temperature are not clear.

DYNAMIC SUPERHELICITY The dynamic methods discussed so far have focused exclusively on the evolution toward mechanical equilibrium of closed, initially circular structures of fixed, nonzero linking differences. But this does not address the question of how the linking differences became nonzero in the first place. Processes that alter DNA topology *in vivo* are inherently dynamic in character, so that, although studies of equilibrium conformations, and dynamic approaches to those conformations at fixed superhelicity, are potentially valuable, dynamic modeling of DNA supercoiling in a nonequilibrium context must include loading processes that dynamically change DNA superhelicity. A well-known example of

such a process is transcription within a torsionally constrained domain. In 1987, Liu & Wang (94) proposed the “transcription-induced twin-supercoiled-domain” model to explain several features characterizing transcriptionally active plasmids; in particular, the observation that high degrees of positive or negative supercoiling of intracellular pBR322 DNA accompany inhibition of DNA gyrase or topoisomerase I, respectively. In this model, illustrated in Figure 5, rotation of RNA polymerase (RNAP) around the helical template during transcription is hindered, for example, by viscous drag, producing a localized torque that leads instead to rotation of the template. If the template is topologically constrained, for instance, owing to anchoring of its ends to intracellular structures, this torque can generate substantial positive supercoiling ahead of the transcription ensemble and negative supercoiling behind it. There is now substantial experimental evidence for such a scenario (reviewed, e.g., in Reference 95).

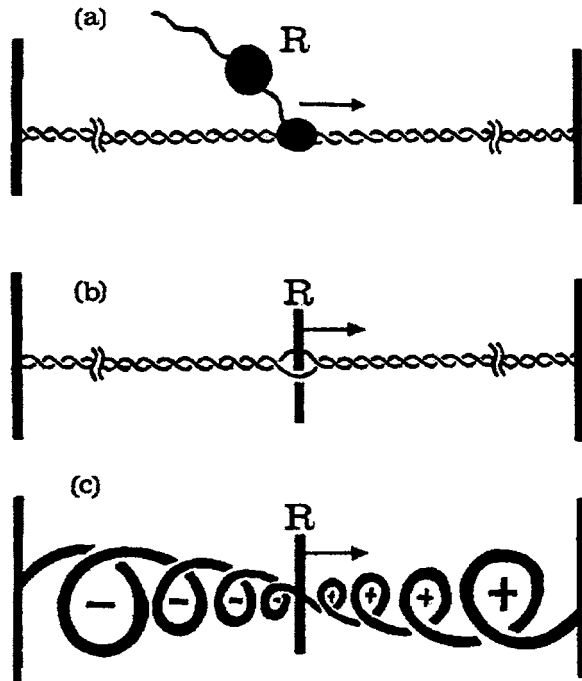


Figure 5 Schematic illustration of transcriptional twin-loop formation (adapted from figure 1 in Reference (94)). (a) A transcription ensemble, R , tracks from left to right along a linear DNA template, both ends of which are anchored, torsionally constraining the domain. (b) If R is rotationally hindered, for instance, owing to anchoring or viscous drag in the intracellular environment, transcription exerts a localized torque upon the template, represented by the vertical bar in the center of the figure. (c) Because the domain is topologically constrained, this torque simultaneously generates positive supercoils downstream and negative supercoils upstream from transcription.

Recently, Mielke and coworkers (90) have invoked a BD bead-chain formulation to simulate the dynamic twin-supercoiling of a 477 bp region of topologically constrained B-DNA in response to an applied torque of magnitude comparable to that exerted by *Escherichia coli* RNAP during transcription (40, 96). These simulations successfully capture the salient features of twin-domain formation, and illuminate a number of general features characterizing the dynamically driven supercoiling of a torsionally relaxed domain, including (a) superhelical stress manifests principally as torsional deformation at early times, as imposed twist propagates through the structure; (b) thereafter, an approximately constant amount of evenly distributed twist is maintained, and additional imposed stress manifests as a slow rise in writhe, until localized buckling results in plectonemic supercoiling; (c) the introduced stress continues to be apportioned approximately exclusively to writhe, resulting in additional supercoiling; until (d) the structure ultimately reaches mechanical equilibrium with the torsional load, and writhe too is maintained at a level approximately constant on average out to late times. These results demonstrate the feasibility of dynamically modeling, within a framework that approximates physiological conditions, nonequilibrium scenarios in which superhelicity itself is time-dependent.

CONCLUSIONS AND OPEN QUESTIONS

Determinants of Superhelical DNA Structure

All the mechanics-based models of superhelical DNA structure developed to date, as long as they do not exclude self-contacts, predict interwound conformations. This is equally true of analyses of stable mechanical equilibria, dynamics of fluctuations or of introduced supercoils, or statistical mechanical analyses—even those that cannot be said to converge to the equilibrium distribution. This uniform conclusion also agrees with virtually all experimental data on solution or EM conformations of superhelical DNA. This strong concordance stands in stark contrast to the predictions of thermodynamic parameters made by these same theories, some of which find entropies associated to superhelicity that have both wrong magnitude and opposite sign from their experimentally measured values. One might conclude that, although the existing mechanics-based theories of DNA structure accurately capture conformational information, they do not reflect the real energetics underlying superhelicity. To propose a resolution of this discrepancy, we first consider the assumptions implicit in these analyses.

All the models developed to date make large simplifications regarding the actual structure of DNA. In some cases, the molecule is modeled as a succession of straight segments, or as beads, with bending confined to the joints between them. In other analyses, specifically those of mechanical equilibrium, much more detail can be incorporated. DNA can be regarded as continuously deformable with an explicitly helical structure, and sequence variations of both structure and mechanical

properties can be included. But even these conditions greatly simplify the actual structure of DNA, which experiments find to be a highly flexible molecule. There are six single covalent bonds between the phosphorous atom on one base and that of its nearest neighbor, five of which allow unrestrained rotations in the absence of steric clashes. At the atomic scale this allows many degrees of freedom that are not included in any existing mechanical analyses of DNA structure. Moreover, interactions with the aqueous solvent are very important determinants of DNA structure that also are not explicitly considered. Indeed, the primary factor stabilizing the double helix is base stacking to exclude water. And DNA orders the water molecules in its immediate neighborhood. Some of the closest water molecules, found in the grooves of the helix, occur so uniformly at specific positions that they appear in crystal structures (so-called crystallographic water). Then the grooves are filled with partially ordered water, which participates in the motions of the molecule and may impart to it more symmetric mechanical properties than the structure of the double helix would suggest. Further out there are hydration shells of partially ordered water around the DNA helix that fade with distance into bulk solvent. Small changes of local DNA conformation may cause large changes in the ensemble of states that the water molecules can assume in response. For these reasons solvent (and ionic) effects are very important determinants of DNA structure that can profoundly influence the thermodynamics, and particularly the entropy, associated to DNA deformations. None of these factors are explicitly included in existing models of DNA structure or mechanics.

All the mechanics-based analyses of DNA structure and superhelicity, whether mechanical, statistical, or dynamic, use experimentally measured values for the mechanical and structural parameters of DNA. However, there are disagreements regarding the precise nature of these mechanical properties, the bending and torsional stiffnesses, and hence also of the elastic and superhelical energies determined therefrom. Is elastic energy an internal energy, that is an enthalpy, or is it a free energy? Landau & Lifshitz (26) and Gray & Hearst (28) assume the latter, whereas other investigators assume the former. Although we do not propose a resolution, we note that each measured stiffness is a single number that is distilled from an experiment in which the DNA and its entrained ions and hydration shells are sampling a very large number of conformational microstates. Thus the measured stiffness is not a property of a single conformation, but of a distribution among states. So, for example, to measure an effective bending energy associated to a particular value of curvature, one in fact is finding some sort of ensemble average over all states of the DNA, water, and ions that is consistent with that amount of overall curvature. Because the accommodation of the ions and solvent to this conformational change are included, this suggests that the bending energy one finds should contain entropic terms; it should be a free energy.

To our knowledge, only the experiments of Gray & Hearst (28) have investigated how the bending stiffness of linear DNA is partitioned between entropic and enthalpic components. No comparable information is available regarding the DNA torsional stiffness. In this regard, single-molecule experiments will only help

if they deform the DNA in a manner comparable to that in which it is deformed in solution. And to evaluate free energies, these deformed states must differ infinitesimally from equilibrium throughout whatever deformation is imposed.

All theoretical analyses that have considered the question have found the entropy of superhelicity to be negative, whereas all experiments find it to be positive. We suggest that this discrepancy arises because these analyses do not determine the full entropy, but only the configurational entropy of supercoiling. They use a highly simplified, jointed segment model of DNA structure in which only its large-scale conformation is explicitly examined, and that often in a simplistic way. It is intuitively clear that interwound DNA is constrained to sample a more confined set of states than is relaxed DNA. So the configurational entropy of plectonemic supercoiling is expected to be negative, as all calculations have shown that it is. But the fact that the experimentally determined entropy of superhelicity is positive clearly indicates that these large-scale deformations are not the primary determinants of the thermodynamics of superhelicity. This reinforces the view that full understanding of superhelical DNA mechanics and energetics will require much more explicit, atomic-scale models.

And yet, all theoretical analyses performed to date correctly predict interwound structures. This occurs despite the fact that the models used are simplistic, do not correctly reproduce the governing thermodynamics, and in some cases even appear to contain errors. Moreover, the experimental evidence regarding the structure of superhelical DNA in solution also points to interwound structures. Clearly interwound conformations must be very robustly stable structures to be so virtually universal.

We suggest that the occurrence of interwound structures is determined more by topology than by energetics or mechanics. To see this, note that, if the DNA duplex were able pass through itself it would change Lk by ± 2 , depending on the sign of the passage. So suppose the DNA has some conformational preference for the relaxed state, the nature of which is not now specified. If $Lk \neq Lk_0$, the relaxed state is not attainable, although the molecule will still strive to reach it. Thus for example, at linking difference $Lk - Lk_0 = \alpha = -2$, the molecule will be found in a figure eight shape because it strives to make the single self-crossing that would return it to the relaxed state. Because this self-crossing is topologically forbidden, the molecule abides in this configuration. At more negative linking differences the molecule simply interwinds further because more self-passages are required to reach the relaxed state.

This scenario is consistent with the conclusion from linear mechanical analyses that it is the forces of self-contact which stabilize interwound structures. Yet the same scenario would occur under much more general conditions. Virtually any hyperelastic mechanics, linear or otherwise, homogeneous or sequence dependent, symmetric or not, would produce the same qualitative behavior, provided the minimum energy state was relaxed. Indeed, one may speculate that even dissipative models would give much the same behavior. At the most extreme, suppose there were no enthalpy associated to DNA deformations at all, and the only driving

factor was the configurational entropy. Because this is negative, the resulting free energy of superhelicity would be positive. So configurational entropy alone could drive DNA toward the relaxed state, which can only be achieved by self-passage. Because this is topologically forbidden in a ccDNA, the molecule will tend to occur predominantly in states of self-contact, which will be interwound supercoils.

If this view is correct, then interwound configurations would result virtually regardless of what mechanical and energetic properties DNA might have. So agreement between the predictions of a model and experimental results would not by itself constitute strong evidence for the correctness of that model. However, if the model correctly predicts more detailed attributes of the distribution of interwound states that may vary among models (such as branching frequency, average supercoil diameter or axis length, distributions between T_w and W_r , etc.), such agreement could be viewed as corroborative.

ACKNOWLEDGMENTS

This work was supported in part by grants DBI 99-04549 and 04-16764 from the National Science Foundation, and RO1-HG01973 and RO1-GM68903 from the National Institutes of Health, and by additional support from the Diversa Corporation. S.P. Mielke, whose work was performed under the auspices of the U.S. Department of Energy by the University of California, Lawrence Livermore National Laboratory, under Contract No. W-7405-Eng-48, acknowledges the University of California, Lawrence Livermore National Laboratory and UC Davis, for continuing support through the Student Employee Graduate Research Fellowship (SEGRF).

**The Annual Review of Biomedical Engineering is online at
<http://bioeng.annualreviews.org>**

LITERATURE CITED

1. Avery OT, MacLeod CM, McCarty M. 1944. Studies on the chemical nature of the substance inducing transformation of pneumococcal types. *J. Exp. Med.* 79:137–58
2. Watson JD, Crick FHC. 1953. A structure of deoxyribose nucleic acid. *Nature* 171:737–38
3. Wollman EL, Jacob F, Hayes W. 1956. Conjugation and genetic recombination in *Escherichia coli* K-12. *Cold Spring Harbor Symp. Quant. Biol.* 21:141
4. Cairns J. 1963. The chromosome of *Escherichia coli*. *Cold Spring Harbor Symp. Quant. Biol.* 28:43–45
5. Fiers W, Sinsheimer RL. 1962. The structure of the bacteriophage ϕ X-174. III. Ultracentrifugal evidence for a ring structure. *J. Mol. Biol.* 5:424–34
6. Weil R, Vinograd J. 1963. The cyclic helix and cyclic coil forms of polyoma viral DNA. *Proc. Natl. Acad. Sci. USA* 50:730–38
7. Vinograd J, Lebowitz J, Radloff R, Watson R, Laipis P. 1965. The twisted circular form of polyoma viral DNA. *Proc. Natl. Acad. Sci. USA* 53:1104–11
8. Lebowitz J. 1990. Through the looking glass: the discovery of supercoiled DNA. *Trends Biochem. Sci.* 15:202–7
9. Vinograd J, Lebowitz J. 1966. Physical and

- topological properties of circular DNA. *J. Gen. Physiol.* 49:103–25
10. Epple M. 1998. Orbits of asteroids, a braid, and the first link invariant. *Math. Intell.* 20:45–52
 11. Calugareanu G. 1961. Sur les classes d'isotopie des noeuds tridimensionnels et leurs invariants. *Czechoslov. Math. J.* 11: 588–625
 12. Pohl W. 1968. The self-linking number of a closed space curve. *J. Math. Mech.* 17:975–86
 13. White J. 1969. Self-linking and the Gaussian integral in higher dimensions. *Am. J. Math.* 91:693–728
 14. Fuller FB. 1971. The writhing number of a space curve. *Proc. Natl. Acad. Sci. USA* 68:815–19
 15. Fuller FB. 1978. Decomposition of the linking number of a closed ribbon: a problem from molecular biology. *Proc. Natl. Acad. Sci. USA* 75:3557–61
 16. Pulleyblank D, Shure M, Tang D, Vinograd J, Vosberg H-P. 1975. Action of nicking-closing enzyme on supercoiled and non-supercoiled closed circular DNA: formation of a Boltzmann distribution of topoisomers. *Proc. Natl. Acad. Sci. USA* 72:4280–84
 17. Boles TC, White JH, Cozzarelli NR. 1990. Structure of plectonemically supercoiled DNA. *J. Mol. Biol.* 213:931–51
 18. Adrian M, Heggeler-Bordier B, Wahli W, Stasiak AZ, Stasiak A, Dubochet J. 1990. Direct visualization of supercoiled DNA molecules in solution. *EMBO J.* 9:4551–54
 19. Bednar J, Furrer P, Stasiak A, Dubochet J. 1994. The twist, writhe and overall shape of supercoiled DNA change during counterion-induced transition from a loosely to a tightly interwound superhelix. *J. Mol. Biol.* 235:825–47
 20. Brady G, Foos D, Benham CJ. 1984. Evidence for an interwound form of the superhelix in circular DNA. *Biopolymers* 23:2963–66
 21. Kirkwood JG, Riseman J. 1948. The intrinsic viscosities and diffusion constants of flexible macromolecules in solution. *J. Chem. Phys.* 16:565–73
 22. Kratky O, Porod G. 1949. Röntgenuntersuchung gelöster Fagenmoleküle. *Rec. Trav. Chim. Pays-Bas* 68:1106–23
 23. Gray HB Jr, Bloomfield VA, Hearst JE. 1967. Sedimentation coefficients of linear and cyclic wormlike coils with excluded-volume effects. *J. Chem. Phys.* 46:1493–98
 24. Bloomfield VA. 1968. Hydrodynamic properties of DNA. *J. Polym. Sci.: Macromol. Rev.* 3:255–316
 25. Eisenberg H. 1969. On the inherent flexibility of DNA chains. *Biopolymers* 8:545–51
 26. Landau LD, Lifshitz EM. 1958. *Statistical Physics*. London: Pergamon Press
 27. Harris RA, Hearst JE. 1966. On polymer dynamics. *J. Chem. Phys.* 44:2595–602
 28. Gray HB Jr, Hearst JE. 1968. Flexibility of native DNA from the sedimentation behavior as a function of molecular weight and temperature. *J. Mol. Biol.* 35:111–29
 29. Schellman JA. 1974. Flexibility of DNA. *Biopolymers* 13:217–26
 30. Bloomfield VA, Crothers DM, Tinoco I Jr. 1974. *Physical Chemistry of Nucleic Acids*. New York: Harper & Row Publ.
 31. Benham CJ. 1977. Elastic model of supercoiling. *Proc. Natl. Acad. Sci. USA* 74: 2397–401
 32. Benham CJ. 1979. An elastic model of the large-scale structure of duplex DNA. *Biopolymers* 18:609–23
 33. Benham CJ. 1983. Geometry and mechanics of DNA superhelicity. *Biopolymers* 22:2477–95
 34. Barkley M, Zimm BH. 1979. Theory of twisting and bending of chain macromolecules: analysis of the fluorescence depolarization of DNA. *J. Chem. Phys.* 70: 2991–3007
 35. Shore D, Baldwin RL. 1983. Energetics of DNA twisting. II. Topoisomer analysis. *J. Mol. Biol.* 170:983–1007
 36. Horowitz DS, Wang JC. 1984. Torsional rigidity of DNA and length dependence of

- the free energy of DNA supercoiling. *J. Mol. Biol.* 173:75–91
37. Smith SB, Finzi L, Bustamante C. 1992. Direct mechanical measurements of the elasticity of single DNA molecules by using magnetic beads. *Science* 258:1122–26
 38. Bustamante C, Marko JF, Siggia ED, Smith SB. 1994. Entropic elasticity of λ -phage DNA. *Science* 265:1599–600
 39. Strick TR, Allemand JF, Bensimon D, Bensimon A, Croquette V. 1996. The elasticity of a single supercoiled DNA molecule. *Science* 271:1835–37
 40. Wang MD, Schnitzer MJ, Yin H, Landick R, Gelles J, Block SM. 1998. Force and velocity measured for single molecules of RNA polymerase. *Science* 282:902–7
 41. Bustamante C, Bryant Z, Smith SB. 2003. Ten years of tension: single-molecule DNA mechanics. *Nature* 421:423–27
 42. Bryant Z, Stone MD, Gore J, Smith SB, Cozzarelli NR, Bustamante C. 2003. Structural transitions and elasticity from torque measurements on DNA. *Nature* 424:338–41
 43. Olson WK, Gorin AA, Lu X-J, Hock LM, Zhurkin VB. 1998. DNA sequence-dependent deformability deduced from protein-DNA crystal complexes. *Proc. Natl. Acad. Sci. USA* 95:11163–68
 44. Bauer WR, Vinograd J. 1970. Interaction of closed circular DNA with intercalative dyes. II. The free energy of superhelix formation in SV40 DNA. *J. Mol. Biol.* 47:419–35
 45. Depew R, Wang JC. 1975. Conformational fluctuations of DNA helix. *Proc. Natl. Acad. Sci. USA* 72:4275–79
 46. Bauer WR, Benham CJ. 1993. The free energy, enthalpy and entropy of native and of partially denatured closed circular DNA. *J. Mol. Biol.* 234:1184–96
 47. Lee CH, Mizusawa H, Kakefuda T. 1981. Unwinding of double-stranded DNA helix by dehydration. *Proc. Natl. Acad. Sci. USA* 78:2838–42
 48. Seidl A, Hinz HJ. 1984. The free energy of DNA supercoiling is enthalpy-determined. *Proc. Natl. Acad. Sci. USA* 81:1312–16
 49. Duguet M. 1993. The helical repeat of DNA at high temperature. *Nucleic Acids Res.* 21:463–68
 50. LeBret M. 1978. Relationship between the energy of superhelix formation, the shear modulus and the torsional Brownian motion of DNA. *Biopolymers* 17:1939–55
 51. LeBret M. 1984. Twist and writhing on short circular DNAs according to first-order elasticity. *Biopolymers* 23:1835–67
 52. Shi Y, Borovik AE, Hearst JE. 1995. Elastic rod model incorporating shear and extension, generalized nonlinear Schrödinger equations, and novel closed-form solutions for supercoiled DNA. *J. Chem. Phys.* 103:3166–83
 53. Manning RS, Maddocks JH, Kahn JD. 1996. A continuum rod model of sequence-dependent DNA structure. *J. Chem. Phys.* 105:5626–46
 54. Coleman BD, Olson WK, Swigon D. 2003. Theory of sequence-dependent DNA elasticity. *J. Chem. Phys.* 118:7127–40
 55. Moakher M, Maddocks JH. 2005. A double-strand elastic rod theory. *Arch. Rat. Mech. Anal.* In press
 56. LeBret M. 1979. Catastrophic variation of twist and writhing of circular DNAs with constraint? *Biopolymers* 18:1709–25
 57. Benham CJ. 1989. Onset of writhe in circular elastic polymers. *Phys. Rev. A* 39:2582–86
 58. Zajac EE. 1962. Stability of two planar loop elasticas. *J. Appl. Mech.* 29:136–42
 59. Bauer WR, Lund RA, White JH. 1993. Twist and writhe of a DNA loop containing intrinsic bends. *Proc. Natl. Acad. Sci. USA* 90:833–37
 60. Manning RS, Rogers KA, Maddocks JH. 1998. Isoperimetric conjugate points with application to the stability of DNA minicircles. *Proc. R. Soc. London A* 454:3047–74
 61. Furrer PB, Manning RS, Maddocks JH. 2000. Rings with multiple energy minima. *Biophys. J.* 79:116–36

62. Yang Y, Tobias I, Olson WK. 1993. Finite element analysis of DNA supercoiling. *J. Chem. Phys.* 98:1673–86
63. Tobias I, Swigon D, Coleman BD. 2000. Elastic stability of DNA configurations. I. General theory. *Phys. Rev. E* 61:747–58
64. Coleman BD, Swigon D, Tobias I. 2000. Elastic stability of DNA configurations. II. Supercoiled plasmids with self-contact. *Phys. Rev. E* 61:759–70
65. Chirico G, Langowski J. 1994. Kinetics of DNA supercoiling studied by Brownian dynamics simulation. *Biopolymers* 34:415–33
66. Klapper I. 1996. Biological applications of the dynamics of twisted elastic rods. *J. Comp. Phys.* 125:325–37
67. Dichmann DJ, Li Y, Maddocks JH. 1996. Hamiltonian formulations and symmetries in rod mechanics. See Ref. 97, pp. 71–113
68. Rouse PE Jr. 1953. A theory of the linear viscoelastic properties of dilute solutions of coiling polymers. *J. Chem. Phys.* 21:1272–80
69. Zimm BH. 1956. Dynamics of polymer molecules in dilute solution: viscoelasticity, flow birefringence and dielectric loss. *J. Chem. Phys.* 24:269–78
70. Hearst JE, Stockmayer WE. 1962. Sedimentation constants of broken chains and wormlike coils. *J. Chem. Phys.* 37:1425–33
71. Klenin KV, Vologodskii AV, Anshelevich VV, Dykhne AM, Frank-Kamenetskii MD. 1991. Computer simulation of DNA supercoiling. *J. Mol. Biol.* 217:413–19
72. Vologodskii AV, Levene SD, Klenin KV, Frank-Kamenetskii M, Cozzarelli NR. 1992. Conformational and thermodynamic properties of supercoiled DNA. *J. Mol. Biol.* 227:1224–43
73. Metropolis N, Rosenbluth AW, Rosenbluth MN, Teller AH, Teller E. 1953. Equation of state calculations by fast computing machines. *J. Chem. Phys.* 21:1087–92
74. Hearst JE, Hunt NG. 1991. Statistical mechanical theory for the plectonemic DNA supercoil. *J. Chem. Phys.* 95:9322–27
75. Marko JF, Siggia ED. 1994. Fluctuations and supercoiling of DNA. *Science* 265:506–8
76. Schlick T, Olson WK. 1992. Supercoiled DNA energetics and dynamics by computer simulation. *J. Mol. Biol.* 223:1089–119
77. Schlick T, Olson WK. 1992. Trefoil knotting revealed by molecular dynamics simulations of supercoiled DNA. *Science* 257:1110–15
78. Schlick T, Li B, Olson WK. 1994. The influence of salt on DNA energetics and dynamics. *Biophys. J.* 67:2446–66
79. Ramachandran G, Schlick T. 1995. Solvent effects on supercoiled DNA dynamics explored by Langevin dynamics simulations. *Phys. Rev. E* 51:6188–203
80. van Gunsteren WF, Berendsen HJC, Rullmann JAC. 1981. Stochastic dynamics for molecules with constraints: Brownian dynamics of n-alkanes. *Mol. Phys.* 44:69–95
81. Dahlquist G, Björck Å. 1974. *Numerical Methods*. Englewood Cliffs, NJ: Prentice-Hall
82. Allison SA, Austin R, Hogan M. 1989. Bending and twisting dynamics of short linear DNAs. *J. Chem. Phys.* 90:3843–54
83. Chirico G. 1996. Torsional-bending infinitesimal dynamics of a DNA chain. *Biopolymers* 38:801–11
84. Iniesta A, Garcia de la Torre J. 1990. A second-order algorithm for the simulation of the Brownian dynamics of macromolecular models. *J. Chem. Phys.* 92:2015–18
85. Hagerman PJ, Zimm BH. 1981. *Biopolymers* 20:1481–502
86. Ermak DL, McCammon JA. 1978. Brownian dynamics with hydrodynamic interactions. *J. Chem. Phys.* 69:1352–60
87. Klenin KV, Merlitz H, Langowski J. 1998. A Brownian dynamics program for the simulation of linear and circular DNA and other wormlike polyelectrolytes. *Biophys. J.* 74:780–88
88. Chirico G, Langowski J. 1996. Brownian dynamics simulations of supercoiled DNA with bent sequences. *Biophys. J.* 71:955–71
89. Huang J, Schlick T. 2002. Macroscopic modeling and simulations of supercoiled

- DNA with bound proteins. *J. Chem. Phys.* 117:8573–86
90. Mielke SP, Fink WH, Krishnan VV, Gronbech-Jensen N, Benham CJ. 2004. Transcription-driven twin supercoiling of a DNA loop: a Brownian dynamics study. *J. Chem. Phys.* 121:8104–12
91. Tabor M, Klapper I. 1996. Dynamics of twist and writhe and the modeling of bacterial fibers. See Ref. (97), pp. 139–59
92. Hou TY, Klapper I, Si H. 1998. Removing the stiffness of curvature in computing 3-D filaments. *J. Comp. Phys.* 143:628–64
93. Klapper I, Qian H. 1998. Remarks on discrete and continuous large-scale models of DNA dynamics. *Biophys. J.* 74:2504–14
94. Liu LF, Wang JC. 1987. Supercoiling of the DNA template during transcription. *Proc. Natl. Acad. Sci. USA* 84:7024–27
95. Wang JC. 1996. DNA topoisomerases. *Annu. Rev. Biochem.* 65:635–92
96. Nelson P. 1999. Transport of torsional stress in DNA. *Proc. Natl. Acad. Sci. USA* 96:14342–47
97. Mesirov JP, Schulten K, Sumners DW, eds. 1996. *Mathematical Approaches to Biomolecular Structure and Dynamics*. New York: Springer-Verlag



CONTENTS

FRONTISPIECE, <i>Werner Goldsmith</i>	xii
WERNER GOLDSMITH: LIFE AND WORK (1924–2003), <i>Stanley A. Berger, Albert I. King, and Jack L. Lewis</i>	1
DNA MECHANICS, <i>Craig J. Benham and Steven P. Mielke</i>	21
QUANTUM DOTS AS CELLULAR PROBES, <i>A. Paul Alivisatos, Weiwei Gu, and Carolyn Larabell</i>	55
BLOOD-ON-A-CHIP, <i>Mehmet Toner and Daniel Irimia</i>	77
BIOCHEMISTRY AND BIOMECHANICS OF CELL MOTILITY, <i>Song Li, Jun-Lin Guan, and Shu Chien</i>	105
MOLECULAR MECHANICS AND DYNAMICS OF LEUKOCYTE RECRUITMENT DURING INFLAMMATION, <i>Scott I. Simon and Chad E. Green</i>	151
DETERMINISTIC AND STOCHASTIC ELEMENTS OF AXONAL GUIDANCE, <i>Susan Maskery and Troy Shinbrot</i>	187
STRUCTURE AND MECHANICS OF HEALING MYOCARDIAL INFARCTS, <i>Jeffrey W. Holmes, Thomas K. Borg, and James W. Covell</i>	223
INSTRUMENTATION ASPECTS OF ANIMAL PET, <i>Yuan-Chuan Tai and Richard Laforest</i>	255
IN VIVO MAGNETIC RESONANCE SPECTROSCOPY IN CANCER, <i>Robert J. Gillies and David L. Morse</i>	287
FUNCTIONAL ELECTRICAL STIMULATION FOR NEUROMUSCULAR APPLICATIONS, <i>P. Hunter Peckham and Jayme S. Knutson</i>	327
RETINAL PROSTHESIS, <i>James D. Weiland, Wentai Liu, and Mark S. Humayun</i>	361
INDEXES	
Subject Index	403
Cumulative Index of Contributing Authors, Volumes 1–7	413
Cumulative Index of Chapter Titles, Volumes 1–7	416
ERRATA	
An online log of corrections to <i>Annual Review of Biomedical Engineering</i> chapters may be found at http://bioeng.annualreviews.org/	